Rifaximin enhances the L-carnitine-mediated preventive effects on skeletal muscle atrophy in cirrhotic rats by modulating the gut-liver-muscle axis

KOJI MURATA, KOSUKE KAJI, NORIHISA NISHIMURA, MASAHIDE ENOMOTO,
YUKI FUJIMOTO, SOICHI TAKEDA, YUKI TSUJI, YUKIHISA FUJINAGA, HIROAKI TAKAYA,
HIDETO KAWARATANI, TADASHI NAMISAKI, TAKEMI AKAHANE and HITOSHI YOSHIJI

Department of Gastroenterology, Nara Medical University, Kashihara, Nara 634-8521, Japan

Abstract. The gut-liver-muscle axis is associated with the development of sarcopenia in liver cirrhosis. The present study aimed to illustrate the combined effects of rifaximin and L-carnitine on skeletal muscle atrophy in cirrhotic rats with steatohepatitis. For this purpose, a total of 344 Fischer rats were fed a choline-deficient L-amino acid-defined (CDAA) diet with the daily oral administration of rifaximin (100 mg/kg) and/or L-carnitine (200 mg/kg), and measurements of psoas muscle mass index and forelimb grip strength were performed. After feeding for 12 weeks, blood samples, and liver, ileum and gastrocnemius muscle tissues were harvested. The effects of L-carnitine on rat myocytes were assessed using *in vitro* assays. Treatment with rifaximin attenuated hyperammonemia and liver fibrosis in the CDAA-fed rats. Moreover, it improved intestinal permeability with the restoration of tight junction proteins and suppressed the lipopolysaccharide (LPS)-mediated hepatic macrophage activation and pro-inflammatory response. In addition, rifaximin prevented skeletal muscle mass atrophy and weakness by decreasing intramuscular myostatin and pro-inflammatory cytokine levels. Moreover, rifaximin synergistically enhanced the L-carnitine-mediated improvement of skeletal muscle wasting by promoting the production of insulin-like growth factor-1 and mitochondrial biogenesis, resulting in the inhibition of the ubiquitin-proteasome system (UPS). The *in vitro* assays revealed that L-carnitine directly attenuated the impairment of mitochondrial biogenesis, thereby inhibiting the UPS in rat myocytes that were stimulated with LPS or tumor necrosis factor-α. On the whole, the present study demonstrates that the combination of rifaximin with L-carnitine may provide a clinical benefit for liver cirrhosis-related sarcopenia.

Introduction

Sarcopenia has been well-established to have a harmful clinical impact on malnutrition in patients with advanced-stage chronic liver disease, and has been implicated in the poor quality of life and negative prognostic outcomes of patients with cirrhosis (1-3). Although sarcopenia varies in prevalence due to different definitions and diagnostic methods, it has been estimated to affect up to 70% of patients with cirrhosis (4,5). Liver cirrhosis-based skeletal muscle wasting invokes a multifactorial pathogenesis, including malnutrition; hyperammonemia; changes in the levels of hormones, including insulin growth factor-1 (IGF-1); chronic inflammation; increased resting energy expenditure; and decreased physical activity (1,2,6-10). Notably, the tripartite inter-organ crosstalk between the gut, liver and skeletal muscle (i.e., the gut-liver-muscle axis) has recently been suggested to contribute to the development of sarcopenia in patients with cirrhosis (11). Therefore, the identification of therapeutic targets for sarcopenia in patients with cirrhosis has often been laborious.

L-carnitine or β-hydroxy-g-N-trimethyl aminobutyric acid is an endogenous molecule involved in the β-oxidation of fatty acids and is biosynthesized from the amino acids, L-lysine and L-methionine, within the brain, kidneys and liver (12). L-carnitine is known to play a key role in cellular energy metabolism through the mitochondrial transport of long-chain fatty acids (13). Clinically, the supplementation of L-carnitine has been suggested to forestall skeletal muscle loss through its anti-inflammatory and antioxidant effects (14,15). Moreover, recent studies have demonstrated that L-carnitine has the potential to prevent the progression of sarcopenia, by attenuating hyperammonemia in patients with cirrhosis (16,17). Although monotherapy with L-carnitine supplementation appears to ameliorate the impairment of muscle mass and function, this is partial and insufficient. Therefore, combining L-carnitine with another agent may prove to be more practical for treating sarcopenia accompanied by liver cirrhosis.

Correspondence to: Dr Kosuke Kaji, Department of Gastroenterology, Nara Medical University, 840 Shijo-cho, Kashihara, Nara 634-8521, Japan
E-mail: kajik@naramed-u.ac.jp

Rifaximin, which is a minimally-absorbed antibiotic with a broad-spectrum activity against aerobic and anaerobic Gram-positive and -negative bacteria, has been clinically used to attenuate hyperammonemia in patients with cirrhosis and hepatic encephalopathy (HE) (18-20). Notably, a recent study that used a model of preclinical sarcopenia in cirrhosis with portosystemic shunts revealed that the rifaximin-mediated decrease in ammonia levels had the potential to reverse skeletal muscle loss (21). Moreover, previous clinical and basic studies by the authors have demonstrated that rifaximin can improve gut hyperpermeability and prevent hepatic exposure to endogenous lipopolysaccharide (LPS), which plays a detrimental role in skeletal muscle homeostasis (22,23). However, the effects of rifaximin and L-carnitine on skeletal muscle atrophy, as well as the underlying mechanisms that are particularly associated with the modulation of the gut-liver-muscle axis, remain obscure.

The present study thus aimed to investigate the combined effects of rifaximin and L-carnitine supplementation on skeletal muscle atrophy and explored the therapeutic mechanisms associated with the gut-liver-muscle axis in a rodent model of cirrhosis.

Materials and methods

Animals and treatment. Fischer 344 rats (6 weeks old, male; body weight, 150±20 g; CLEA Japan) were randomly divided into five groups and treated for 12 weeks as follows (Fig. 1A; n=10 in each group): i) With a choline-sufficient amino acid-defined (CSAA) diet (Research Diets, Inc.) with lactose hydrate (FUJIFILM, Wako Pure Chemical Corporation) as the vehicle; ii) with a choline-deficient l-amino acid-defined (CDAA) diet (Research Diets Inc.) with the vehicle; iii) with the CDAA diet with rifaximin (ASKA Pharmaceutical Co. Ltd.; 100 mg/kg); iv) with the CDAA diet and L-carnitine (Otsuka Pharmaceutical Co. Ltd.; 200 mg/kg); and v) with the CDAA diet with rifaximin and L-carnitine, as previously described (23,24). All drugs were administered by intragastric gavage once a day. The rats were housed in plastic cages (2 rats/cage) in a pathogen-free room and were provided with free access to their diet and drinking water, and were kept under controlled, stable ambient conditions (23±3˚C/12-h light/dark cycle with 50±20% humidity). At the end of the experiment, all rats underwent the following procedures: Euthanasia by an intraperitoneal injection of pentobarbital sodium (200 mg/kg), the opening of the abdominal cavity, blood collection via puncture of the aorta and harvesting of the liver, ileum and gastrocnemius muscle for histological and molecular evaluation. The anesthetized rats were then decapitated for assuring death. The present study was approved by the Animal Ethics Committee of Nara Medical University (approval no. 12764), and all protocols were performed in accordance with the National Institutes of Health Guidelines for the Care and Use of Laboratory Animals.

Rat myoblast culture. L6 rat skeletal muscle myoblasts (cat. no. JCRB9081, Japanese Collection of Research Bioresources Cell Bank) were cultured and differentiated into myotubes as previously described (25,26). Briefly, the cells were cultured in Dulbecco's modified Eagle's medium (DMEM, Nacalai Tesque,

Inc.) supplemented with 10% fetal bovine serum (Gibco; Thermo Fisher Scientific, Inc.) and antibiotics (1% penicillin and streptomycin) at 37˚C in a 5% CO_2 air environment. To induce differentiation into myocytes, the cells were further cultured in DMEM containing 2% horse serum for 8 days. The cells were supplemented with fresh medium every 48 h and were used at the stage of myotubes (60-70%) (25,27,28). Myogenic differentiation into myotubes was confirmed by using a AE2000-1080M microscope (Shimadzu Corporation) based on the morphological alignment, elongation and fusion (data not shown). Mycoplasma testing was performed using a MycoProbe® Mycoplasma Detection kit (R&D Systems, Inc.) according to the manufacturer's protocol. The differentiated myotubes were stimulated with LPS (O55:B5; MilliporeSigma) or tumor necrosis factor-α (TNF-α) at various concentrations and treated with LPS (1.0 μg/ml) or TNF-α (20 ng/ml) and L-carnitine (5 mM) and/or rifaximin (10 μM) for 48 h.

Measurement of psoas muscle mass index (PMI) and forelimb grip strength. According to the clinical criteria for sarcopenia assessment, the PMI (cross-sectional area/height^2) was assessed on a single computed tomography (CT) slice (image) at the level of the L3 pedicle using Slice-O-Matic (Tomovision) (29). All rats underwent an abdominal CT scan before and at 4, 8, and 12 weeks after the start of CDAA feeding and/or rifaximin/L-carnitine treatment using CosmoScan FX (Rigaku Corporation) as previously described (26). The forelimb grip strength of the experimental rats was simultaneously measured using a grip strength meter (MK-380Si; Muromachi Kikai, Co., Ltd.) as previously described (26). During the grip strength test, the rats were allowed to use their front paws to grab a horizontal bar mounted on the gauge, and the tail was slowly pulled back. The peak tension was recorded at the time the mouse released the grip on the bar. Measurements were repeated three times, and the mean of three measurements was recorded.

Serum alanine aminotransferase (ALT) and albumin measurement in rats. The serum ALT and albumin concentrations in the rats were measured using a Rat Alanine Aminotransferase ELISA kit (cat. no. ab285264, Abcam) and Rat Albumin ELISA kit (cat. no. ab108789, Abcam), respectively. All samples were processed and assayed according to the manufacturer's protocol.

Serum and hepatic IGF-1 measurement in rats. The serum IGF-1 concentrations in the rats were measured using a Mouse/Rat IGF-I/IGF-1 Quantikine ELISA kit (cat. no. MG100, R&D Systems, Inc.). All samples were processed and assayed according to the manufacturer's protocol.

Plasma and muscle ammonia measurement. The concentrations of ammonia in plasma and muscle (100 mg of rat gastrocnemius muscle tissue homogenate) were measured using the Ammonia Assay kit (cat. no. ab83360, Abcam), according to the manufacturer's protocol.

Hepatic triglyceride (TG) concentration. The intrahepatic TG concentrations in 100 mg frozen liver tissue per mouse were measured using the Triglyceride-Glo™ Assay (Promega Corporation), according to the manufacturer's instructions.
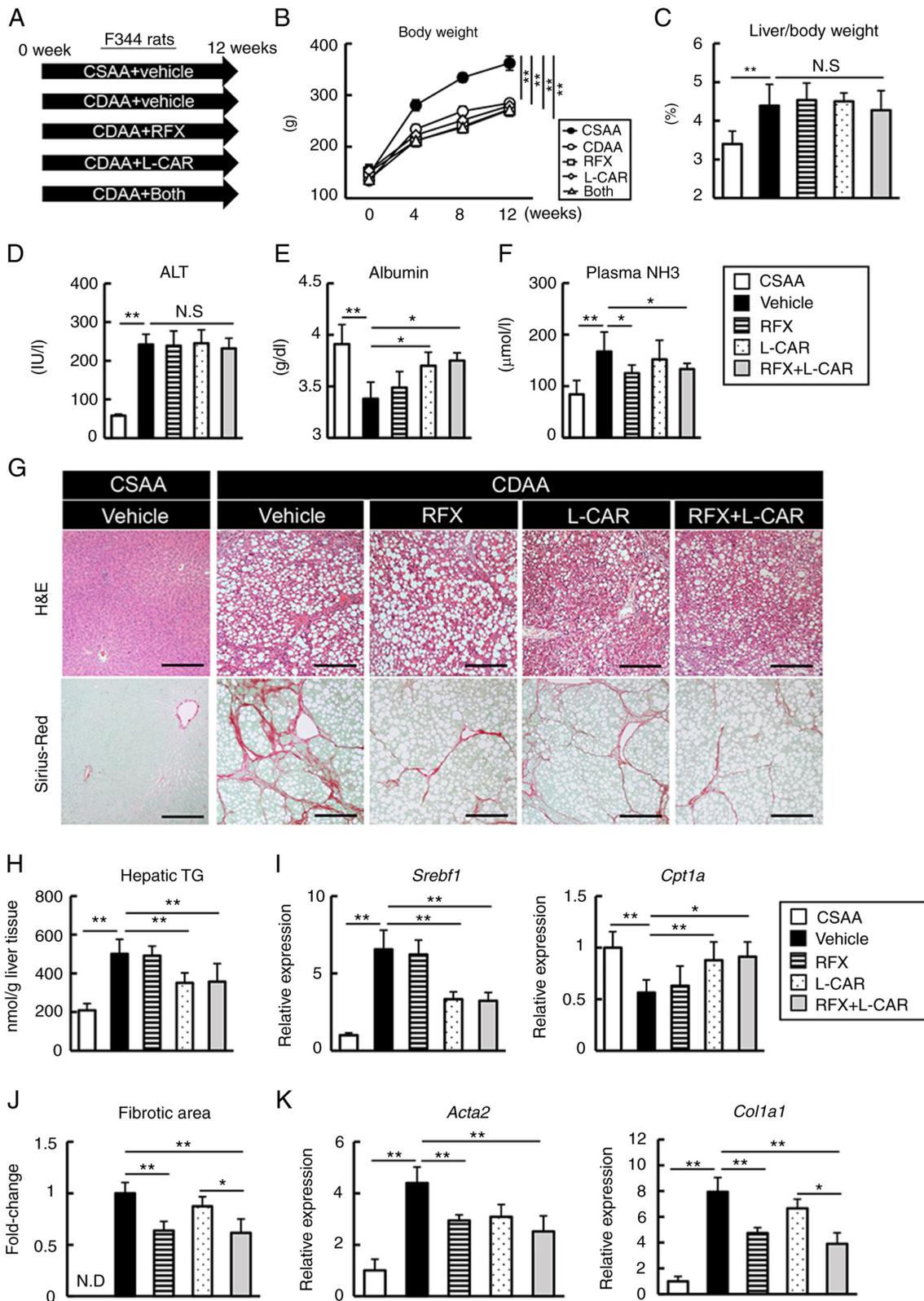
Figure 1. Effects of rifaximin and L-carnitine on hepatic phenotypes in CDAA-fed rats. (A) Experimental protocols. (B) Changes in the body weight of the rats during the experimental period. The comparison was performed between the groups at the last time point. (C) Ratio of liver weight to body weight at the end of the experiment. (D-F) Blood levels of ALT, albumin and NH3. (G) Representative microphotographs of liver sections stained with H&E and Sirius Red in the experimental groups. Scale bar, 50 μm. (H) Hepatic concentrations of TG. (I) Relative mRNA expression levels of *Srebf1* and *Cpt1a* in the liver of experimental rats. (J) Semi-quantification of Sirius Red-stained fibrotic area in high-power field using ImageJ software. (K) Relative mRNA expression levels of *Acta2* and *Col1a1* in the livers of experimental rats. The mRNA expression levels were measured using reverse transcription-quantitative PCR, and *Gapdh* was used as an internal control. Histochemical quantitative analyses included five fields per section. (I-K) Quantitative values are indicated as fold changes relative to the values of CSAA group. Data are the mean ± SD (n=10), *P<0.05 and **P<0.01, significant difference between groups. N.S, not significant; N.D, not detected; CDAA, choline-deficient L-amino acid-defined diet; CSAA, choline-sufficient amino acid-defined diet; ALT, alanine aminotransferase; NH3, ammonia; H&E, hematoxylin and eosin; TG, triglycerides; RFX, rifaximin; L-CAR, L-carnitine; *Srebf1*, sterol regulatory element binding transcription factor 1; *Cpt1a*, carnitine palmitoyltransferase 1A; *Acta2*, actin alpha 2, smooth muscle; *Col1a1*, collagen type i alpha 1 chain.

Rat muscle myostatin measurements. The levels of myostatin in 100 mg rat gastrocnemius muscle tissue homogenate were measured using a myostatin ELISA kit (cat. no. DGDF80, R&D Systems, Inc.) following the manufacturer's instructions.

Measurement of in vivo intestinal permeability. A 4-kDa fluorescein isothiocyanate (FITC)-dextran (MilliporeSigma) solution was used for the intestinal permeability measurement, as previously described (30). Another set of rats (n=5) in each group was applied to evaluate *in vivo* intestinal permeability. Briefly, 6 h after initiating fasting conditions (only fasted from food), FITC-dextran was gently administered via oral gavage to the rats at 40 mg/kg, 200 μl body weight. Blood was collected from the portal vein at 1 h after the FITC-dextran administration. To evaluate the degree of gut permeability, blood was analyzed by the fluorescence measurement of the concentration of FITC-labeled dextran at an excitation wavelength of 490 nm and an emission wavelength of 520 nm using a NanoDrop 3300 fluorospectrometer (Thermo Fisher Scientific, Inc.).

Histological, immunohistochemical and immunofluorescent analyses. The liver, ileum and gastrocnemius specimens were fixed in 10% formalin, incubated overnight at room temperature and embedded in paraffin. Sections of 5-μm thickness were stained with hematoxylin and eosin (H&E) and Sirius Red (performed at Narabyouri Research Co., Nara, Japan). For immunohistochemical staining, the liver tissue sections were blocked with 10% goat serum (Abcam) for 30 min following deparaffinization and antigen retrieval, and then incubated overnight at 4˚C with mouse-monoclonal CD68 antibody (1:100; cat. no. GTX41868, GeneTex, Inc.). The sections were washed three times with phosphate-buffered saline and subsequently incubated with a goat anti-mouse IgG (H+L) HRP-conjugated secondary antibody (1:2,000; cat. no. 62-6520, Thermo Fisher Scientific, Inc.) for 30 min at room temperature. The slides were developed with DAB until the signal clearly appeared, and the nuclei were stained with hematoxylin for 5 min at room temperature, and images were obtained using a BX53 microscope (Olympus Corporation).

For immunofluorescence, the ileum sections were deparaffinized and rehydrated and blocked in a similar manner to immunohistochemical staining, and then rabbit-polyclonal Zonula occludens-1 (ZO-1; 1:100; cat. no. 61-7300, Invitrogen; Thermo Fisher Scientific, Inc.) and rabbit-polyclonal Occludin (1:100; cat. no. 71-1500, Invitrogen; Thermo Fisher Scientific, Inc.) were used as primary antibodies. Following overnight incubation at 4˚C, the immunofluorescence detection of the primary antibodies was performed using goat anti-rabbit IgG (H+L) Alexa Fluor-conjugated secondary antibodies (1:200; cat. nos. R37116 and A-21207, Thermo Fisher Scientific, Inc.) for 1 h at room temperature. The sections were mounted on Vectashield mounting medium with 4',6-diamidino-2-phenylindole Fluoromount-G mounting medium for fluorescent nucleic acid staining (Vector Laboratories, Inc.) and images were captured using a BZ-X700 microscope (Keyence Corporation). Semi-quantitative analysis was performed for five fields per section in high-power fields at x400 magnification using ImageJ software version 64 (National Institutes of Health).

RNA extraction and reverse transcription-quantitative polymerase chain reaction (RT-qPCR). Total RNA was isolated from the liver and muscle tissues and cultured rat L6 myocyte cells. The RNeasy Mini kit (Qiagen GmbH) was used for the liver tissues and L6 cells, and the RNeasy Fibrous Tissue Mini kit (Qiagen GmbH) was used for the muscle tissues. The RNA samples were then treated with DNase in order to remove DNA contamination with TURBO DNA-free™ DNase (Invitrogen; Thermo Fisher Scientific, Inc.) and total RNA (2 μg) was reverse transcribed into complementary DNA (cDNA) using the High-Capacity RNA-to-cDNA kit (Applied Biosystems; Thermo Fisher Scientific, Inc.) by applying the following three stages: 37˚C for 15 min, 85˚C for 5 sec and then cooling at 4˚C. qPCR was performed using the primer pairs listed in Table SI, and SYBR™-Green PCR Master Mix (Applied Biosystems; Thermo Fisher Scientific, Inc.), and an Applied Biosystems StepOnePlus™ Real-Time PCR® system (Applied Biosystems; Thermo Fisher Scientific, Inc.). The thermocycling conditions were as follows: 95˚C for 5 min, followed by 40 cycles of 95˚C for 10 sec, 60˚C for 20 sec and then 72˚C for 20 sec; melting at 95˚C for 5 sec, 65˚C for 60 sec and 97˚C for 1 sec and cooling at 40˚C for 10 sec. Relative expression was normalized to *Gapdh* expression, and estimated using the $2^{-\Delta\Delta Cq}$ method, and presented as the fold change relative to the control (31).

Protein extraction and western blot analysis. Whole cell lysate proteins were extracted from the intestinal and muscle tissues, and cultured rat L6 myocyte cells using tissue-protein extraction reagent (T-PER) supplemented with proteinase and phosphatase inhibitors (all from Thermo Fisher Scientific, Inc.). The protein concentration was measured using a protein assay (Bio-Rad Laboratories, Inc.). In total, 50 μg whole cell lysates were separated by sodium dodecyl sulfate-polyacrylamide gel electrophoresis (NuPAGE™ 4-12%, Bis-Tris; Thermo Fisher Scientific, Inc.) and transferred to Invitrolon polyvinylidene difluoride membranes (Thermo Fisher Scientific, Inc.), which were subsequently blocked for 1 h with 5% bovine serum albumin (Thermo Fisher Scientific, Inc.) in Tris-buffered saline supplemented with Tween-20 (Cell Signaling Technology, Inc.). The membranes were then incubated overnight at 4˚C with antibodies against rabbit-polyclonal ZO-1 (1:500; cat. no. 61-7300) and rabbit-polyclonal Occludin (1:125; cat. no. 71-1500) (from Invitrogen; Thermo Fisher Scientific, Inc.), p70S6K (1:1,000, cat. no. 9202), phosphorylated (p-) p70S6K (Thr389; 1:1,000, cat. no. 9205), nuclear factor-κB (NF-κB) p65 (1:1,000, cat. no. 8242), p-NF-κB p65 (Ser536; 1:1,000, cat. no. 3033), GAPDH (1:1,000, cat. no. 2118) and actin (1:1,000, cat. no. 4967) (from Cell Signaling Technology, Inc.). The membranes were washed and incubated at room temperature for 1 h with Amersham ECL horseradish peroxidase-conjugated immunoglobulin G F(ab)2 fragment antibody (1:5,000 dilution; cat. no. NA931, GE Healthcare; Cytiva) and developed using Clarity Western enhanced chemiluminescence substrate (Bio-Rad Laboratories, Inc.). Immunoblotting bands were densitometrically analyzed using ImageJ 64-bit Java 1.8.0 software (National Institutes of Health).

Mitochondrial DNA (mtDNA) copy number. Total DNA was obtained from the gastrocnemius muscle tissue using a DNA Extractor® TIS kit (FUJIFILM, Wako Pure Chemical Corporation). The mtDNA copy number was assessed using RT-qPCR as described in above according to mtDNA (*Rnr2*)/nDNA (*Gapdh*). The primer sequences used were as follows: RNR2 forward, 5'-AGCTATTAATGGTTCGTT TGT-3' and reverse, 5'-AGGAGGCTCCATTTCTCTTGT-3'; and nuclear-encoded GAPDH forward, 5'-GGAAAGACAGGT GTTTTGCA-3' and reverse, 5'-AGGTCAGAGTGAGCAGGA CA-3'. The PCR amplification process was as follows: One cycle at 95°C for 10 min, 40 cycles at 95°C for 15 sec and 60°C for 1 min. Both mtDNA and nDNA threshold cycle (CT) average values were obtained, and the mtDNA content was calculated relative to nDNA as mtDNA/nDNA=$2^{(CTnDNA-CTmtDNA)}$.

Mitochondrial respiration and extracellular acidification. The oxygen consumption rate (OCR) was measured using the XFe96 extracellular flux analyzer (Agilent Technologies, Inc.) as previously described (32). Briefly, the L6 cells were seeded at 8,000 cells per well in a 96-well tissue culture plate 24 h before running the flux analyzer. To assess the mitochondrial respiration rate, the cells were incubated in XF base medium (Agilent Technologies, Inc.) supplemented with 10 mM glucose, 1 mM pyruvate and 2 mM glutamine for 1.5 h at 37°C. Subsequently, the OCR was measured following the addition of 1 μM oligomycin to inhibit ATP synthesis from oxidative phosphorylation, 1.5 μM carbonyl cyanide 4-(trifluoromethoxy) phenylhydrazone (FCCP) to uncouple the mitochondrial membrane that stimulates respiration, and a mixture containing 0.5 μM each of antimycin A and rotenone (A+R) to inhibit complex I and III that terminates mitochondrial oxidative phosphorylation. After the seahorse measurements were completed, total cellular content was measured using a CyQUANT Cell Proliferation Assay kit (Thermo Fisher Scientific, Inc.), and the OCR values were normalized to the cellular mitochondrial content (number of cells x mtDNA/nDNA). The basal OCR was calculated as follows: [OCR$_{(initial)}$-OCR$_{(A + R)}$]. The maximum OCR was computed as follows: [OCR$_{(FCCP)}$-OCR$_{(A + R)}$].

Measurement of mitochondrial membrane potential. Tetramethylrhodamine methyl ester (TMRM; FUJIFILM, Wako Pure Chemical Corporation) were used to assess the mitochondrial membrane potential. The L6 cells were stained by addition of the dye to the culture medium at 100 nM for 30 min at 37°C. Subsequently, the cells were stained with the Hoechst 33342 nuclear dye (Thermo Fisher Scientific, Inc.) at a 1:500 dilution in PBS at room temperature for 10 min, washed with PBS, and visualized using a BZ-X700 (Keyence Corporation). The intensity of the fluorescence signal was quantified using ImageJ software version 64 (National Institutes of Health).

Statistical analyses. Statistical analyses were performed using Prism, version 9.1.2 (GraphPad Software, Inc.). Data were analyzed using one-way ANOVA followed by Tukey's test as a post hoc test. Values are presented as the mean ± standard deviation. A value of $P<0.05$ was considered to indicate a statistically significant difference.

Results

Effects of the combined use of rifaximin and L-carnitine on CDAA-induced hepatic steatosis and fibrosis. The experimental design of the study is illustrated in Fig. 1A. The CDAA-fed rats exhibited a significant decrease in body weight and hepatomegaly as compared with the CSAA-fed rats; however, neither rifaximin nor L-carnitine inhibited these physical impairments (Fig. 1B and C). Serological analysis revealed elevated alanine aminotransferase (ALT) levels, as well as a decreased albumin level in the CDAA-fed rats; neither rifaximin nor L-carnitine significantly affected the ALT levels; however, L-carnitine suppressed the progression of hypoalbuminemia (Fig. 1D and E). Rifaximin also mildly improved CDAA-induced hyperammonemia (Fig. 1F). The histological assessment demonstrated that hepatic lipid accumulation in the CDAA-fed rats was suppressed by L-carnitine, but not by rifaximin (Fig. 1G). Concomitantly, treatment with L-carnitine decreased the hepatic TG levels, with the decreased expression of the lipogenesis-related gene, sterol regulatory element binding transcription factor 1 (*Srebf1*), and the increased expression of carnitine palmitoyltransferase 1A (*Cpt1a*) (Fig. 1H and I). Moreover, Sirius Red staining revealed that hepatic fibrosis progression was prevented by rifaximin, which was consistent with the reduced expression mRNA levels of hepatic profibrotic markers [i.e., actin alpha 2, smooth muscle (*Acta2*) and collagen type i alpha 1 chain (*Col1a1*)]; however, these events were not significantly mediated by L-carnitine (Fig. 1G-K).

Rifaximin inhibits the CDAA-induced expansion of hepatic macrophages and the LPS/Toll-like receptor 4 (TLR4)-mediated inflammatory response. Based on the suppression of liver fibrosis following rifaximin treatment, the present study then examined the pro-inflammatory status and the hepatic LPS/TLR4 pathway. The results revealed an extensive hepatic infiltration of CD68-positive macrophages in the CDAA-fed rats, which was attenuated by treatment with rifaximin (Fig. 2A and B). Corresponding with the upregulated expression of hepatic LPS-binding protein (*Lbp*), the mRNA levels of *Tlr4* and its coreceptor, *Cd14*, were increased in the CDAA-fed rats. Notably, treatment with rifaximin inhibited these effects (Fig. 2C and D). In this context, rifaximin treatment significantly reduced the hepatic mRNA levels of pro-inflammatory cytokines, including *Tnfa Il1b* and *Il6* (Fig. 2E). On the other hand, treatment with L-carnitine alone did not affect the inflammatory response (Fig. 2A-E).

Subsequently, the present study assessed the changes in the status of IGF-1, which is a potent myotrophic factor. Both the hepatic and serum concentrations of IGF-1 were decreased in the CDAA-fed rats, compared with the CSAA-fed rats (Fig. 2F and G). It was found that L-carnitine suppressed the CDAA-induced decrease in IGF-1 production (Fig. 2F and G). Of note, combination treatment with L-carnitine and rifaximin effectively enhanced the suppressive effects of L-carnitine on the reduction of the liver and serum IGF-1 levels in the CDAA-fed rats by reducing the LPS overload, which was recognized to suppress the hepatic production of IGF-1 (Fig. 2F and G).
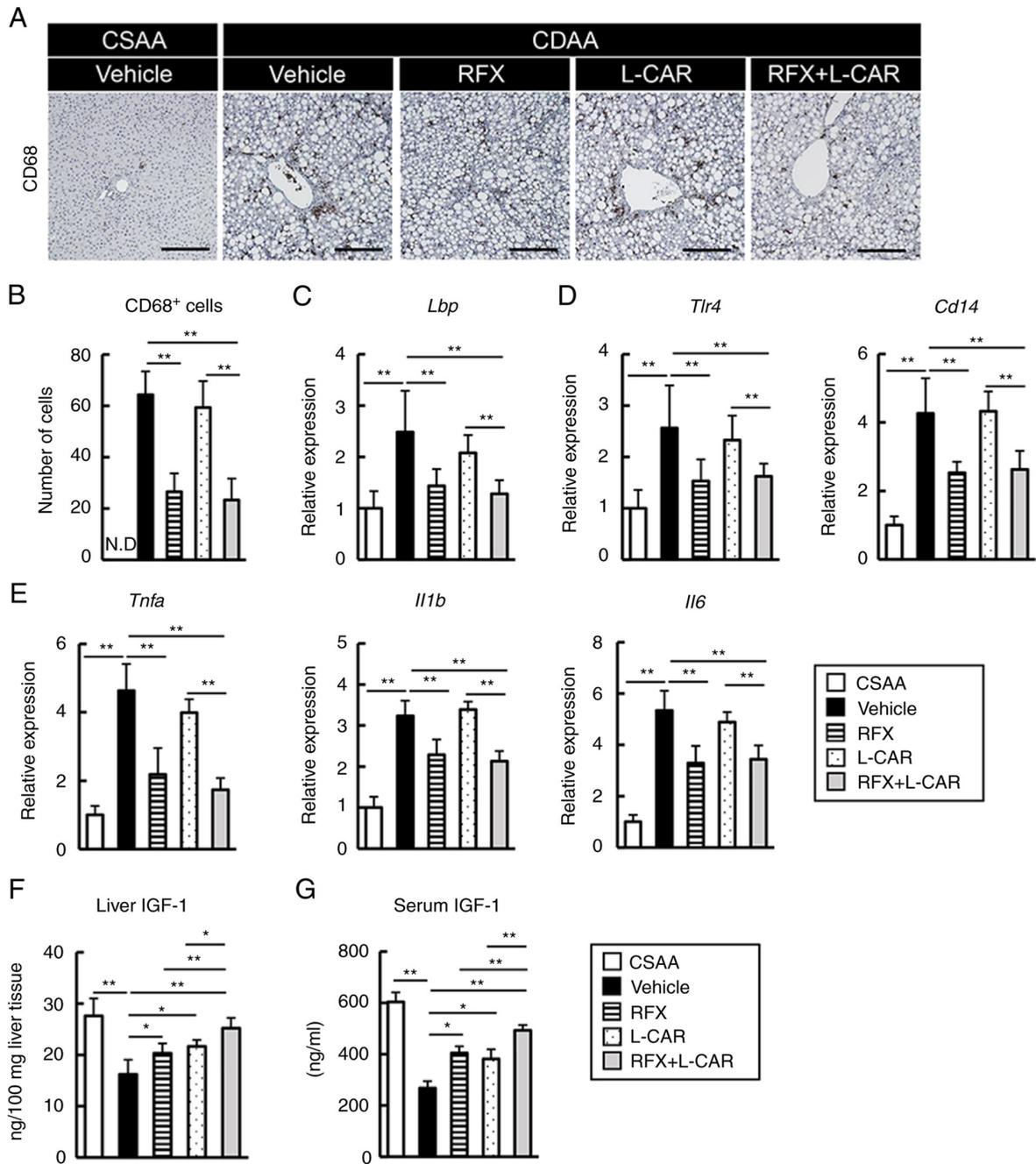
Figure 2. Effects of rifaximin and L-carnitine on the LPS/TLR4-mediated inflammatory response and IGF-1 levels in CDAA-fed rats. (A) Representative microphotographs of liver sections stained with CD68 in the experimental groups. Scale bar, 50 μm. (B) Semi-quantification of CD68-positive cells in a high-power field using ImageJ software. (C-E) Relative mRNA expression level of (C) *Lbp*, (D) *Tlr4* and *Cd14*, *Tnfa*, and (E) *Il1b* and *Il6* in the livers of experimental rats. The mRNA expression levels were measured using reverse transcription-quantitative PCR, and *Gapdh* was used as an internal control. (F and G) Hepatic and serum levels of IGF-1. Data are the mean ± SD (n=10). *P<0.05 and **P<0.01, significant difference between groups. N.D, not detected; LPS, lipopolysaccharide; TLR4, Toll-like receptor 4; *Lbp*, LPS-binding protein; IGF-1, insulin-like growth factor-1; CDAA, choline-deficient L-amino acid-defined diet; CSAA, choline-sufficient amino acid-defined diet; RFX, rifaximin; L-CAR, L-carnitine.

Rifaximin attenuates CDAA-induced intestinal hyperpermeability. To elucidate the functional mechanisms of the rifaximin-mediated prevention of the hepatic overload by endogenous LPS, intestinal permeability was then evaluated. Immunofluorescence staining revealed that the areas that were immuno-positive for ZO-1 and Occludin, the representative markers of tight junction proteins (TJPs), were profoundly less in number in the CDAA-fed group than in the CSAA-fed group; notably, this deprivation of TJPs was effectively restored by

treatment with rifaximin (Fig. 3A-C). The results of western blot analysis supported these findings; rifaximin replenished the TJP protein levels (Fig. 3D and E). In addition, the leakage of plasma FITC-dextran was augmented by >2.5-fold by the CDAA diet and was inversely proportional with the deprivation of TJPs (Fig. 3F). Treatment with rifaximin led to a marked decreased in the leakage of FITC-dextran in the CDAA-fed rats (Fig. 3F). Treatment with L-carnitine alone did not affect the impairment of intestinal barrier function (Fig. 3).
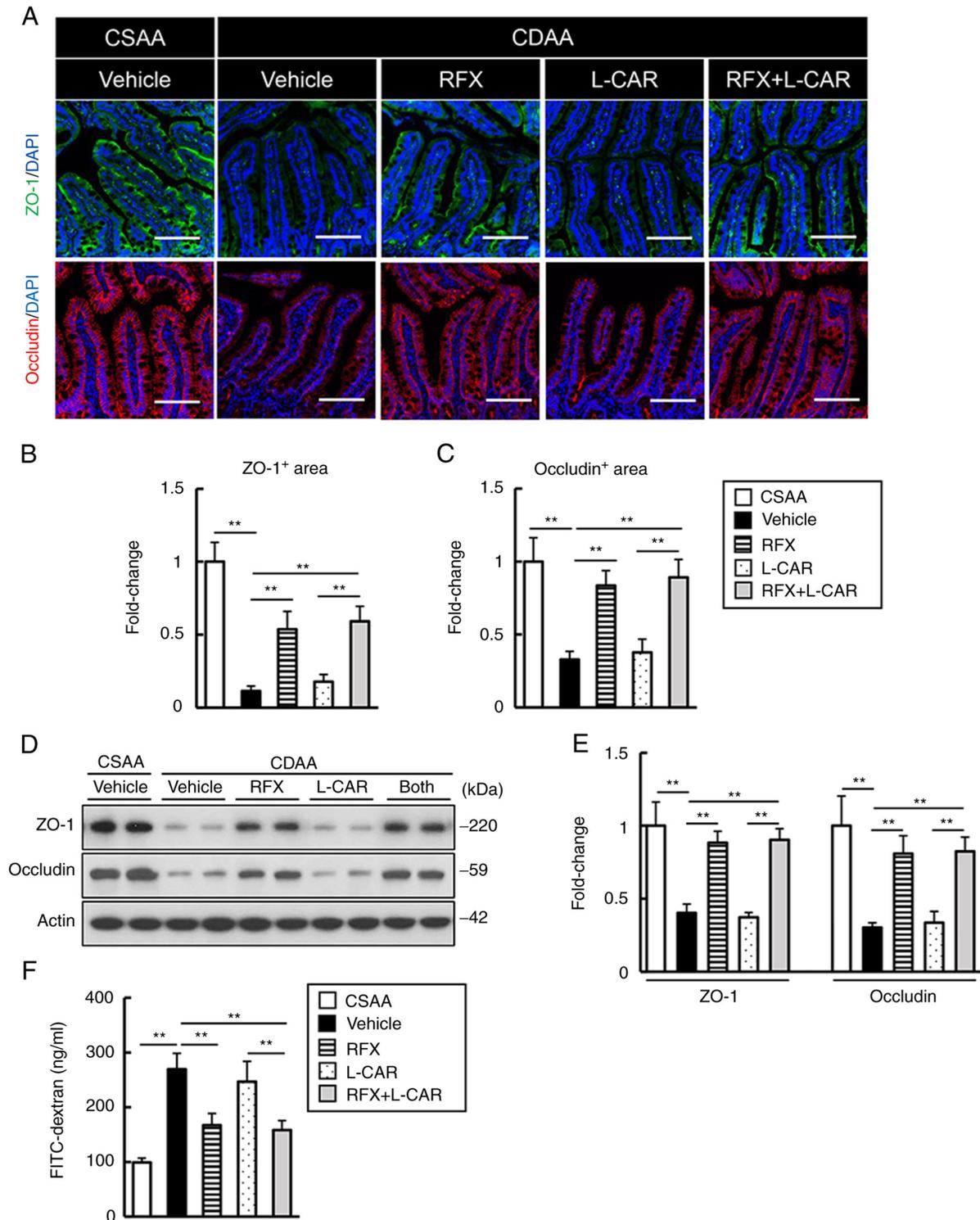
Figure 3. Effects of rifaximin and L-carnitine on intestinal barrier function in CDAA-fed rats. (A) Representative microphotographs of ileum sections stained with ZO-1 and occludin in the experimental groups. Nuclei were counterstained with DAPI. Scale bar, 50 μm. (B and C) Semi-quantification of ZO-1 and occludin immuno-positive areas in a high-power field using ImageJ software. (D) Western blots for ZO-1 and occludin in the ilea of experimental mice. Actin was used as an internal control. (E) Densitometric quantification of the protein expression of ZO-1 and occludin. (F) Blood levels of FITC-dextran (4 kDa) at 4 h after the oral administration. (B, C and E) Quantitative values are indicated as fold changes to the values of CSAA group Data are the mean ± SD. (B and C) n=10, (E) n=4, (F) n=5). **P<0.01, significant difference between groups. ZO-1, zonula occludens-1; CDAA, choline-deficient L-amino acid-defined diet; CSAA, choline-sufficient amino acid-defined diet; RFX, rifaximin; L-CAR, L-carnitine.

Inhibitory effects of rifaximin and L-carnitine on CDAA-induced skeletal muscle atrophy and strength. Considering the marked weight loss of the rats, it was hypothesized that the CDAA-fed rats would undergo skeletal muscle atrophy. After 12 weeks of

feeding, the body length of the rats was significantly shortened in the CDAA-fed group, and rifaximin or L-carnitine treatment did not reverse this change (Fig. 4A and B). After 4 weeks of feeding, the value of PMI, determined as the cross-sectional area/height[2],
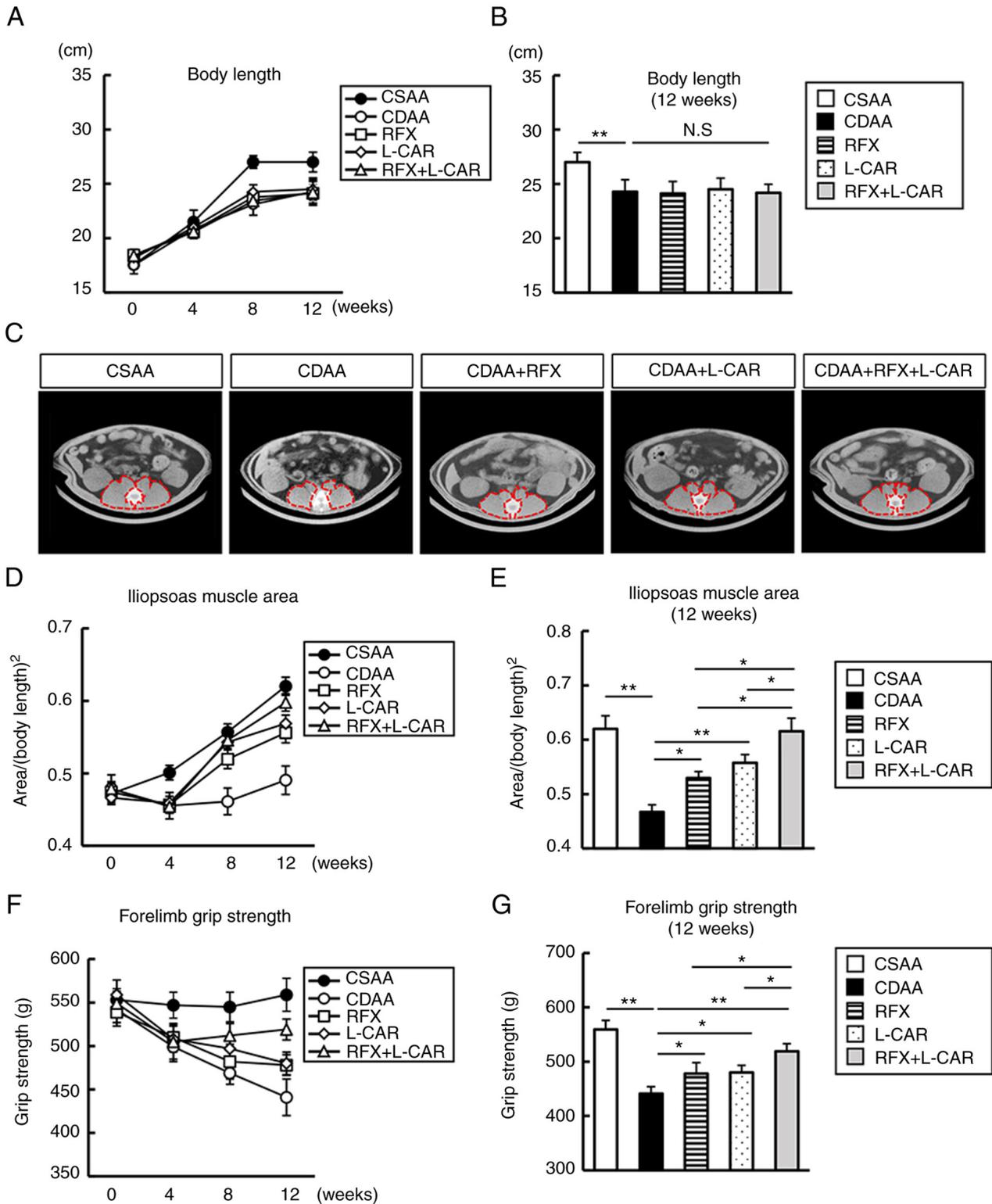
Figure 4. Effects of rifaximin and L-carnitine on skeletal muscle mass and strength in CDAA-fed rats. (A) Changes in body lengths during the experimental period. (B) Body length at 12 weeks of treatment. (C) Representative images of CT slice at the psoas muscle at 12 weeks of treatment. (D) Chronological changes in the calculated PMI (cross sectional area/height^2) during the experimental period. (E) PMI values at 12 weeks of treatment. (F) Chronological changes in the forelimb grip strength during the experimental period. (G) Forelimb grip strength at 12 weeks of treatment. Data are the mean ± SD (n=10). [*]P<0.05 and [**]P<0.01, significant difference between groups. N.S, not significant; PMI, psoas mass index; CDAA, choline-deficient L-amino acid-defined diet; CSAA, choline-sufficient amino acid-defined diet; RFX, rifaximin; L-CAR, L-carnitine.

significantly decreased in the CDAA-fed group (Fig. 4C and D). Notably, rifaximin and L-carnitine suppressed the CDAA-induced decrease in PMI after 8 weeks of treatment, which was enhanced after 12 weeks of combined treatment (Fig. 4C-E).

The present study further investigated the efficacy of both agents on forelimb grip strength. The CDAA diet significantly weakened forelimb grip strength after 4 weeks (Fig. 4F and G). In accordance with the effects observed on muscle atrophy,

monotherapy with rifaximin and L-carnitine prevented the CDAA-induced decrease in forelimb grip strength, and the combination of these agents augmented these preventive effects after 12 weeks (Fig. 4F and G).

Effects of rifaximin and L-carnitine on skeletal muscle protein metabolism in CDAA-fed rats. To elucidate the effects of rifaximin and L-carnitine on skeletal muscle protein metabolism, the changes in protein synthesis and degradation in the gastrocnemius muscle tissues were further analyzed. As illustrated in Fig. 5A-C, the histological assessment of gastrocnemius muscle fiber revealed a marked decrease in fiber length and density in the CDAA-fed group. Treatment with either rifaximin or L-carnitine efficiently ameliorated muscle fiber atrophy, and the combination of both agents potentiated these effects (Fig. 5A-C). The phosphoinositide 3-kinase/Akt/mammalian target of rapamycin (mTOR) pathway is a pivotal process in muscle protein synthesis. In CDAA-fed group, the phosphorylation of intramuscular p70S6K (Thr389), a hallmark of activation by mTOR, was significantly diminished as compared to CSAA-fed group (Fig. 5D and E). This CDAA-induced decrease in p70S6K phosphorylation was suppressed by rifaximin and L-carnitine treatment (Fig. 5D and E).

The present study then evaluated the muscle levels of ammonia and myostatin, which is a myokine that inhibits muscle cell growth. In the CDAA-fed rats, the intramuscular ammonia levels were elevated along with changes in serum ammonia levels; this effect was attenuated by rifaximin treatment (Fig. 5F). Consistently, the marked increase in the myostatin levels in the CDAA-fed rats was suppressed by rifaximin treatment (Fig. 5G). Furthermore, in the CDAA-fed rats, there was an upregulation in the levels of the inflammatory mediators, *Tnfa*, *Il1b* and NLR family pyrin domain containing 3 (*Nlrp3*), following NF-κB activation in the skeletal muscle, and rifaximin potently suppressed the activation of these pro-inflammatory pathways (Fig. 5H-J). These effects were not observed in the muscles of the L-carnitine-treated rats (Fig. 5F-J).

Based on the fact that mitochondrial function dictates muscle fiber homeostasis, the present study investigated mitochondrial biogenesis in the gastrocnemius muscle tissue. The CDAA-fed rats manifested a prominent decrease in the intramuscular levels of mitochondrial biogenesis-related genes, peroxisome proliferator-activated receptor γ coactivator-1α (PGC-1α; *Ppargc1a*) and mitochondrial transcription factor A (TFAM; *Tfam*) (Fig. 5K). Of note, these decreases were efficiently restored by treatment with either rifaximin or L-carnitine; this was augmented by the combination of both agents (Fig. 5K).

Following the changes in these regulatory factors, the intramuscular mRNA expression levels of *Atrogin-1* and muscle RING-finger protein-1 (*MuRF-1*), which are the pivotal markers of the ubiquitin-proteasome system (UPS), were upregulated in the CDAA-fed group; treatment with rifaximin and L-carnitine attenuated these effects (Fig. 5L).

L-carnitine inhibits the LPS- or TNF-α-stimulated impairment of mitochondrial biogenesis and the UPS in skeletal muscle cells. In the model in the present study, it was found that L-carnitine supplementation attenuated the impairment of mitochondrial biogenesis and the progression of UPS in the course of muscle degradation. Therefore, the present study then examined whether L-carnitine could directly affect differentiated L6 rat myotubes *in vitro* (Fig. 6A). As shown in Fig. S1A and B, LPS stimulation decreased the mRNA levels of *Ppargc1a* and *Tfam* in a concentration-dependent manner, and conversely increased those of *Atrogin-1* and *MuRF-1* in rat myotubes. Of note, L-carnitine suppressed the LPS-induced decrease in the levels of mitochondrial biogenesis-related markers, and consequently inhibited the UPS stimulation by LPS (Fig. 6B and C). To further evaluate mitochondrial biogenesis, the cellular mitochondrial content was measured by quantifying mtDNA over nuclear DNA (mtDNA/nDNA). The results revealed a a marked reduction in mtDNA/nDNA in the LPS-stimulated L6 myotubes, and treatment with L-carnitine restored the LPS-stimulated reduction in mtDNA/nDNA (Fig. 6D). Moreover, mitochondrial membrane potential, an indicator of mitochondrial function, was assessed by the fluorescence intensity of TMRM that accumulates in the mitochondria. As shown in Fig. 6E and F, mitochondrial membrane potential was decreased in the LPS-stimulated L6 myotubes, and this decrease was suppressed by treatment with L-carnitine.

Subsequently, the cellular effects of both agents on mitochondrial respiration were examined using seahorse analyses to measure the OCR of L6 myotubes stimulated with LPS. The OCR values were normalized to the cellular mitochondrial content and the basal and maximal respiration rates were calculated. The results revealed that stimulation with LPS downregulated both the basal OCR and maximal respiratory capacity in L6 myotubes, which were restored by treatment with L-carnitine (Fig. 6G and H).

Inflammatory cytokines have been reported to impair intramuscular mitochondrial biogenesis. Thus, the present study also examined the effects of both agents on the TNF-α-induced impairment of mitochondrial biogenesis. TNF-α administration exacerbated the impairment of mitochondrial biogenesis, mitochondrial membrane potential and respiratory capacity and promoted the UPS in the rat myotubes in L6 myotubes (Figs. S1C and D, and S2C-F). Notably, L-carnitine significantly prevented this sequence of muscle degradation induced by TNF-α stimulation (Fig. S2A-F). By contrast, rifaximin did not directly affect myotubes. These findings suggest that L-carnitine reversed the LPS- or TNF-α-induced impairment of mitochondrial biogenesis in myotubes.

Taken together, the results demonstrated that rifaximin enhanced the inhibitory effects of L-carnitine supplementation on skeletal muscle atrophy in CDAA-fed cirrhotic rats via multifunctional mechanisms based on the modulation of the gut-liver-muscle axis (Fig. 7).

Discussion

The present study demonstrated that the additional administration of rifaximin effectively potentiated the preventive effects of L-carnitine supplementation on skeletal muscle wasting in a CDAA-fed rat model. To date, studies have proposed several experimental models of cirrhosis-based sarcopenia in rodents. Giusto *et al* (33) observed skeletal muscle myopenia in both
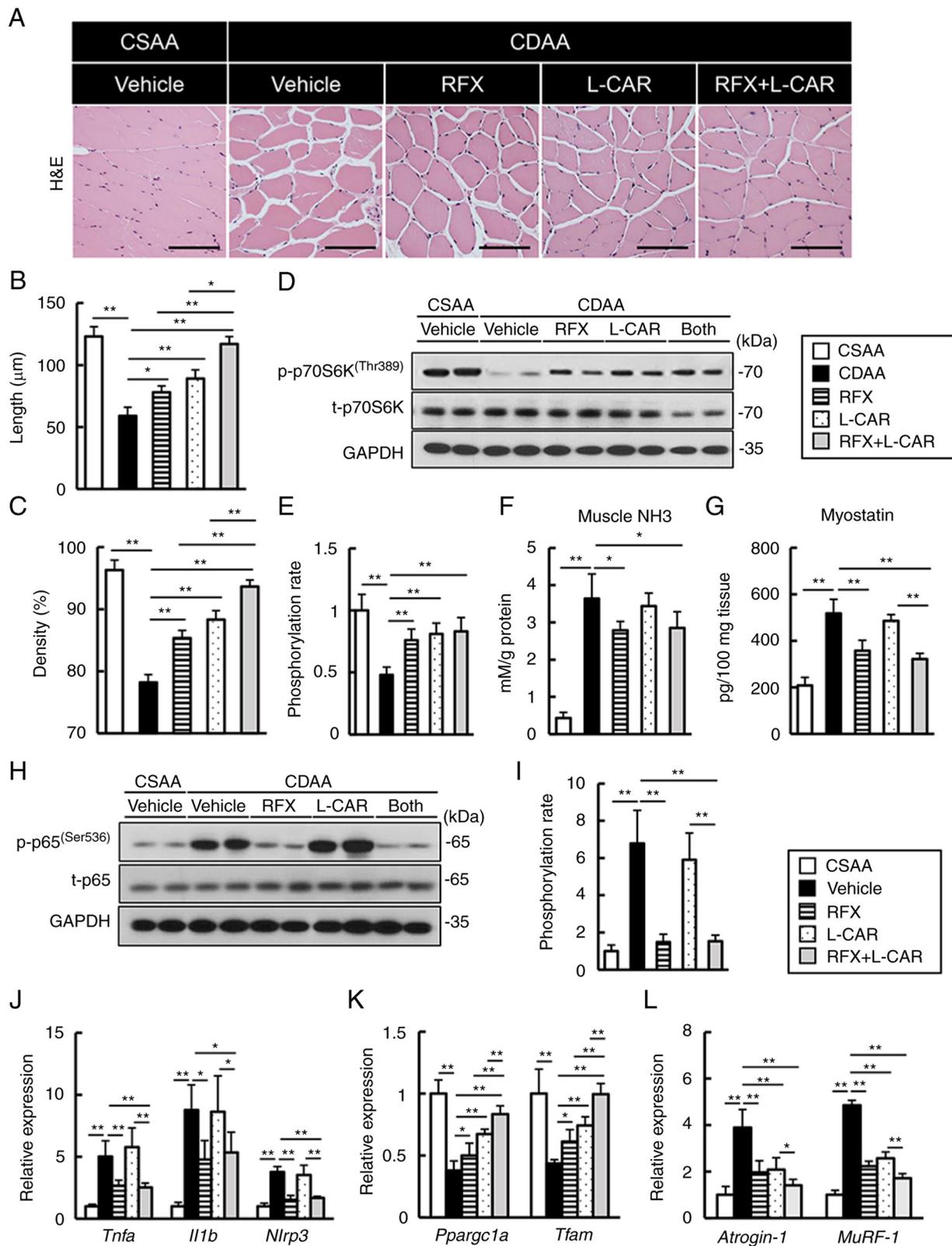
Figure 5. Effects of rifaximin and L-carnitine on protein synthesis and the degradation of gastrocnemius muscle in CDAA-fed rats. (A) Representative microphotographs of gastrocnemius muscle sections stained with H&E in the experimental groups. Scale bar, 50 μm. (B and C) Summary data of myocyte cross-sectional length and density. (D) Western blots for p70S6K phosphorylation in gastrocnemius muscle tissues. (E) Quantification of phosphorylated p70S6K/total p70S6K. (F) Ammonia levels in gastrocnemius muscle tissues of experimental rats. (G) Myostatin concentrations in gastrocnemius muscle tissues of experimental rats. (H) Western blots for NF-κB p65 phosphorylation in gastrocnemius muscle tissues. (I) Quantification of phosphorylated p65/total p65. (J-L) Relative mRNA expression levels of (J) *Tnfa*, *Il1b* and *Nlrp3*, (K) *Ppargc1a* and *Tfam*, and (L) *Atrogin-1* and *MuRF-1* in the gastrocnemius muscle of experimental rats. (D and H) GAPDH was used as the loading control for western blot analysis. The mRNA expression levels were measured using reverse transcription-quantitative PCR and *Gapdh* was used as an internal control. Quantitative values are indicated as fold changes to the values of CSAA group (E-G and I-L). Data are the mean ± SD. (B, C, F, G and J-L) n=10, (E and I) n=4. *P<0.05 and **P<0.01, significant difference between groups. H&E, hematoxylin and eosin; CDAA, choline-deficient L-amino acid-defined diet; CSAA, choline-sufficient amino acid-defined diet; RFX, rifaximin; L-CAR, L-carnitine; *Ppargc1a*, peroxisome proliferator-activated receptor γ coactivator-1α; *Tfam*, mitochondrial transcription factor A; *MuRF-1*, muscle RING-finger protein-1.
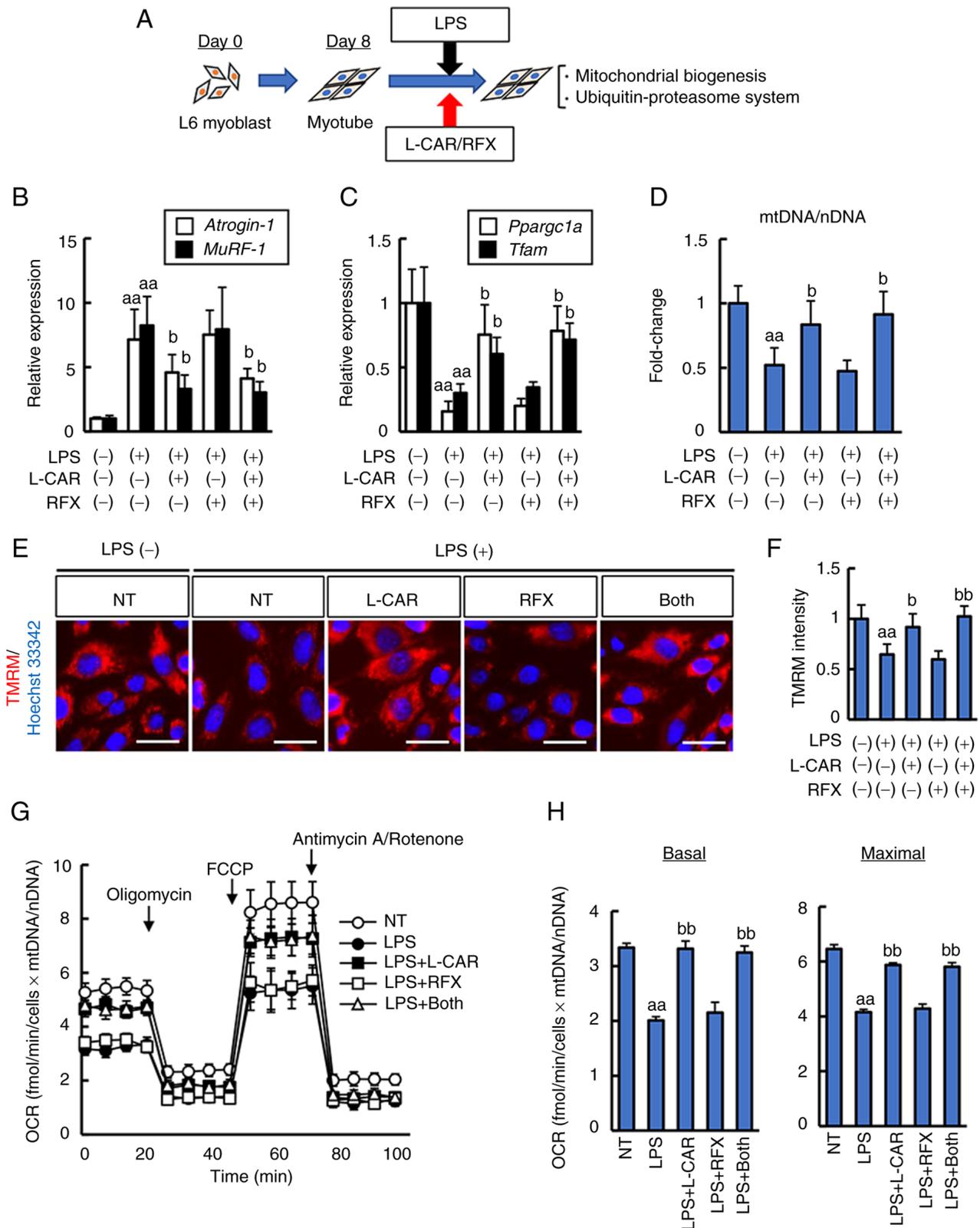
Figure 6. Cellular mitochondrial biogenesis in LPS-stimulated rat L6 myocytes. (A) *In vitro* experimental protocol. (B and C) Effects of L-carnitine and/or rifaximin on the mRNA expression levels of (B) *Atrogin-1* and *MuRF-1*, and (C) *Ppargc1a* and *Tfam* in LPS-stimulated rat L6 myocytes. The mRNA expression levels were measured using reverse transcription-quantitative PCR, and *Gapdh* was used as an internal control. (D) The mitochondrial content was assessed using quantitative PCR as described in the Materias and methods. (E) Representative images of TMRM live stains corresponding to mitochondrial membrane potential. Scale bar, 50 μm. (F) Quantification of TMRM intensity per cell; data shown as the mean ± SD for 100 cells per condition in three representative experiments. Nuclei were stained with Hoechst 33342. (G) Measurements of OCR using a seahorse extracellular flux analyzer. (H) Calculations of the basal and maximal respiration rates. Cells were treated with LPS (1.0 μg/ml) and L-carnitine (5 mM) and/or rifaximin (10 μM) for 48 h. Quantitative values are indicated as fold changes to the values of non-treated (NT) groups (B, C and D). Data are the mean ± SD; (B, C and D) n=8, (F) n=3, or the mean ± SEM (G and H) n=5. [aa]P<0.01 vs. LPS (-)/L-CAR (-)/RFX (-), [b]P<0.05 and [bb]P<0.01 vs. LPS (+)/L-CAR (-)/RFX (-). LPS, lipopolysaccharide; TMRM, tetramethylrhodamine methyl ester; OCR, oxygen consumption rate; CSAA, choline-sufficient amino acid-defined diet; RFX, rifaximin; L-CAR, L-carnitine; *Ppargc1a*, peroxisome proliferator-activated receptor γ coactivator-1α; *Tfam*, mitochondrial transcription factor A; *MuRF-1*, muscle RING-finger protein-1.
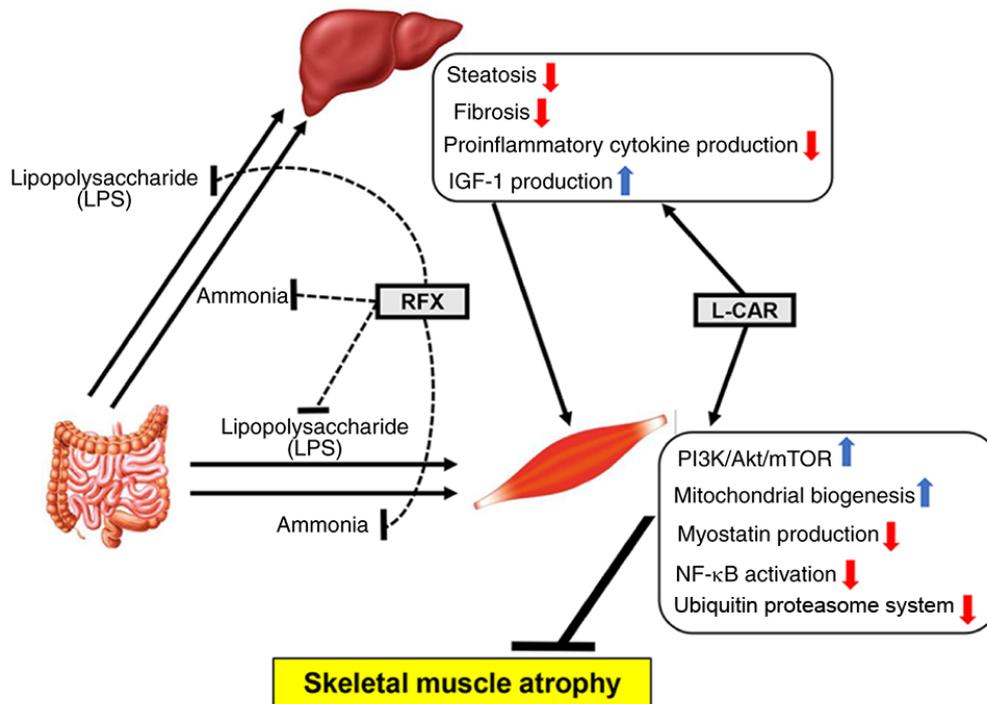
Figure 7. Graphic representation of the effects of rifaximin and L-carnitine on skeletal muscle atrophy in choline-deficient L-amino acid-defined diet-fed cirrhotic rats. RFX, rifaximin; L-CAR, L-carnitine; IGF-1, insulin growth factor-1.

bile duct ligation and carbon tetrachloride-induced cirrhosis. Moreover, choline has been reported to be required for skeletal muscle homeostasis based on its proper modulation of fat and protein metabolism and counteraction of inflammation, apoptosis and autophagy (34). Indeed, a recent study by the authors suggested that CDAA feeding induced marked steatohepatitis and fibrosis, accompanied by significant skeletal muscle atrophy in rats (26). Moreover, it has also been found that CDAA-fed rats exhibit gut hyperpermeability (35). Therefore, this model was assumed to be suitable to address the therapeutic interventions through the gut-liver-muscle axis.

The present study demonstrated that monotherapy with rifaximin exerted an inhibitory effect on the atrophic changes in the skeletal muscle of CDAA-fed rats. In this context, the involvement of multifunctional mechanisms was suggested (Fig. 7). First, rifaximin attenuated hyperammonemia in the CDAA-fed rats according to its pharmacological property. Hyperammonemia has been recognized to trigger skeletal muscle wasting related with liver cirrhosis (1,2). In patients with cirrhosis, muscle ammonia levels are often elevated and can lead to the induction of NF-κB, and thus to a further increase in myostatin expression, followed by the inhibition of myogenesis and an increase in autophagy (36). Likewise, Kumar *et al* (21) reported that combination therapy with rifaximin and L-ornithine L-aspartate reversed sarcopenia in a rat model of portocaval anastomosis by suppressing the GCN2-dependent hyperammonemic cellular stress response. Consistently, the present study demonstrated a reduction in intramuscular ammonia levels, as well as improved hyperammonemia following rifaximin treatment of the CDAA-fed rats. This suggested that lowering the ammonia level partially contributed to the rifaximin-mediated inhibition of the development of sarcopenia. On the other hand, sarcopenia has been noted to be irreversible following liver transplantation despite normal ammonia metabolism in the graft, suggesting that the withdrawal of ammonia alone is insufficient for the recovery of sarcopenia (37). In this respect, rifaximin was likely to more potently attenuate skeletal muscle atrophy than hyperammonemia in the model used herein. Thus, this suggests the possible involvement of another functional mechanism in this anti-myopenic effect.

The present study focused on the impact of rifaximin on the status of endogenous LPS. Endotoxemia is exacerbated due to an impaired intestinal barrier integrity and dysbiosis in liver cirrhosis, particularly when related to alcoholic liver injury and non-alcoholic steatohepatitis (38,39). In line with a previous study by the authors, the rifaximin-mediated blunting of intestinal hyperpermeability suppressed the CDAA-induced hepatic proinflammatory response and fibrogenesis by inhibiting hepatic the LPS/TLR4 signaling pathway (23). Subsequently, the upregulation in the levels of inflammatory mediators was suppressed by rifaximin treatment in skeletal muscle. Given that TNF-α is a key mediator of liver fibrosis-induced muscle atrophy, the rifaximin-mediated anti-sarcopenic effect was also relevant to the improved hepatic pathology (40). Previous studies have documented that an LPS stimulus decreases the circulating levels and hepatic expression of IGF-1, and leads to the inhibition of skeletal muscle protein synthesis (41,42). In the present study, the CDAA-fed rats exhibited a reduction in both serum and hepatic levels of IGF-1 along with the hepatic overload of LPS. Of note, rifaximin significantly suppressed the decrease in the IGF-1 level, corroborating the likelihood that rifaximin could also prevent sarcopenia by shielding from exposure to gut-derived LPS.

The present study underscored the results on the enhanced effect of L-carnitine supplementation on skeletal muscle atrophy with the addition of rifaximin. Previous studies have documented that L-carnitine increases the plasma IGF-1 level and results in the suppression of the UPS-induced myofibrillar protein degradation in humans and rodents (43,44). Consistently, the findings of the present study demonstrated that L-carnitine exerted a limited effect on hepatic and gut phenotypes in the CDAA-fed rats, while it significantly improved lipid metabolism in the liver, increased hepatic and serum levels of IGF-1, and promoted mTOR signaling activation and mitochondrial biogenesis in the skeletal muscle, resulting in the suppression of muscle atrophy. Moreover, the results suggested that L-carnitine increased the levels of key regulators involved in skeletal muscle mitochondrial biogenesis in the CDAA-fed rats. To reflect this, the *in vitro* experiments demonstrated that L-carnitine directly improved mitochondrial biogenesis and oxygen respiratory function, and consequently attenuated the UPS in rat myotubes stimulated with both LPS and TNF-α. Moreover, rifaximin did not directly affect myotubes, suggesting that it predominantly suppressed skeletal muscle atrophy by reducing the exposure of LPS and inflammatory cytokines, as well as ammonia to muscle tissue. These findings strongly suggest that L-carnitine is available as a conventional therapy for cirrhosis-related sarcopenia and that its combined use with rifaximin has the potential to be a novel effective therapy.

The present study had several limitations which should be noted. First, the effect of rifaximin on microbial profiles was obscure in the present model. In this context, previous research has indicated the impact of rifaximin on the gut microbiota. Patel *et al* (45) demonstrated that rifaximin reduced the mucin-degrading sialidase-rich species, leading to gut barrier repair in patients with cirrhosis with HE. Kitagawa *et al* (46) demonstrated that rifaximin attenuated ethanol-induced liver injury in mice followed by a decrease in *Erysipelotrichales* and an increase in *Bacteroidales*. Given these findings, further analyses are required to identify the interaction between microbial alterations by rifaximin and the therapeutic effects in the current model. Second, although the doses of rifaximin (100 mg/kg/day) and L-carnitine (200 mg/kg/day) for use in the *in vivo* experiments were selected based on previous studies (23,24), the results did not disclose that these selected doses were relevant to the clinical dose. The package insert from ASKA Pharmaceutical Co. Ltd. has documented that when rifaximin is used at the dose used in the present study and orally administered to male rats, the maximum plasma concentration is almost equal to that observed with the clinical dose (1,100 mg/day) orally administered to patients with liver cirrhosis for 14 days. Moreover, since rifaximin is a poorly absorbable drug and specifically affects the gastrointestinal tract, it is relatively difficult to determine the dose equivalent to clinical doses by measuring the blood concentration. A previous study demonstrated that the dose of rifaximin (100 mg/kg/day) sufficiently affected the intestine and colon in rats (47). Additionally, it was observed that these doses of both drugs did not exhibit hepatic and renal toxicity in rats (data not shown). Thus, these doses are considered to be within tolerance for use in *in vivo* experiments. However, further pharmacokinetics analyses are required to evaluate whether the doses used in the present study were relevant to the clinical dose. Third, the present study did not observe the suppression of body weight loss in the CDAA-fed rats by treatment with both agents, in spite of the improvement of skeletal muscle atrophy. In this regard, it was hypothesized that both agents would possibly reduce visceral fat, as well as increase skeletal muscle in the CDAA-fed rats. However, this is merely a speculation and further investigations are required to confirm this hypothesis by evaluating the changes in visceral fat following treatment with both agents.

In conclusion, the present study demonstrated that rifaximin enhanced the anti-myopenic properties of L-carnitine supplementation in the skeletal muscle of CDAA-fed rats. Notably, this effect of rifaximin was based on the modulation of the gut-liver-muscle axis through the suppression of the endogenous LPS overload by maintaining intestinal barrier function, in addition to its ammonia-lowering properties. Of note, both drugs are clinically available for patients with chronic liver diseases and that the aforementioned effects on skeletal muscle wasting were achieved without observing any drug toxicity. Therefore, these findings suggested that this combination regimen may provide a clinical benefit for liver cirrhosis-related sarcopenia.

Availability of data and materials

The datasets used and/or analyzed during the current study are available from the corresponding author on reasonable request.

Authors' contributions

KM, KK, TN, TA and HY contributed to the conception and design of the present study. KM, KK, NN, ME, YFujimoto, ST, YT, YFujinaga, HT and HK performed the experiments and analyzed the data. KM, KK and HY wrote and revised the manuscript. KM, KK and NN confirm the authenticity of all the raw data. All authors have read and approved the final manuscript.

Ethics approval and consent to participate

The present study was approved by the Animal Ethics Committee of Nara Medical University (approval no. 12764), and all protocols were performed in accordance with the National Institutes of Health Guidelines for the Care and Use of Laboratory Animals.

Patient consent for publication

Not applicable.

Competing interests

The authors declare that they have no competing interests.

References

1. Dasarathy S and Merli M: Sarcopenia from mechanism to diagnosis and treatment in liver disease. J Hepatol 65: 1232-1244, 2016.
2. Bhanji RA, Montano-Loza AJ and Watt KD: Sarcopenia in cirrhosis: Looking beyond the skeletal muscle loss to see the systemic disease. Hepatology 70: 2193-2203, 2019.
3. Tandon P, Montano-Loza AJ, Lai JC, Dasarathy S and Merli M: Sarcopenia and frailty in decompensated cirrhosis. J Hepatol 75 (Suppl 1): S147-S162, 2021.
4. Vasques J, Guerreiro CS, Sousa J, Pinto M and Cortez-Pinto H: Nutritional support in cirrhotic patients with sarcopenia. Clin Nutr ESPEN 33: 12-17, 2019.
5. Ebadi M, Bhanji RA, Mazurak VC and Montano-Loza AJ: Sarcopenia in cirrhosis: From pathogenesis to interventions. J Gastroenterol 54: 845-859, 2019.
6. Ascenzi F, Barberi L, Dobrowolny G, Villa Nova Bacurau A, Nicoletti C, Rizzuto E, Rosenthal N, Scicchitano BM and Musarò A: Effects of IGF-1 isoforms on muscle growth and sarcopenia. Aging Cell 18: e12954, 2019.
7. Nishikawa H, Enomoto H, Nishiguchi S and Iijima H: Liver cirrhosis and sarcopenia from the viewpoint of dysbiosis. Int J Mol Sci 21: 5254, 2020.
8. West J, Gow PJ, Testro A, Chapman B and Sinclair M: Exercise physiology in cirrhosis and the potential benefits of exercise interventions: A review. J Gastroenterol Hepatol 36: 2687-2705, 2021.
9. Dos Santos ALS and Anastácio LR: The impact of L-branched-chain amino acids and L-leucine on malnutrition, sarcopenia, and other outcomes in patients with chronic liver disease. Expert Rev Gastroenterol Hepatol 15: 181-194, 2021.
10. Sinclair M, Grossmann M, Angus PW, Hoermann R, Hey P, Scodellaro T and Gow PJ: Low testosterone as a better predictor of mortality than sarcopenia in men with advanced liver disease. J Gastroenterol Hepatol 31: 661-667, 2016.
11. Ponziani FR, Picca A, Marzetti E, Calvani R, Conta G, Del Chierico F, Capuani G, Faccia M, Fianchi F, Funaro B, et al: Characterization of the gut-liver-muscle axis in cirrhotic patients with sarcopenia. Liver Int 41: 1320-1334, 2021.
12. Kendler BS: Carnitine: An overview of its role in preventive medicine. Prev Med 15: 373-390, 1986.
13. Houten SM, Wanders RJA and Ranea-Robles P: Metabolic interactions between peroxisomes and mitochondria with a special focus on acylcarnitine metabolism. Biochim Biophys Acta Mol Basis Dis 1866: 165720, 2020.
14. Hanai T, Shiraki M, Imai K, Suetugu A, Takai K and Shimizu M: Usefulness of carnitine supplementation for the complications of liver cirrhosis. Nutrients 12: 1915, 2020.
15. Ohashi K, Ishikawa T, Hoshii A, Hokari T, Suzuki M, Noguchi H, Hirosawa H, Koyama F, Kobayashi M, Hirosawa S, et al: Effect of levocarnitine administration in patients with chronic liver disease. Exp Ther Med 20: 94, 2020.
16. Ohara M, Ogawa K, Suda G, Kimura M, Maehara O, Shimazaki T, Suzuki K, Nakamura A, Umemura M, Izumi T, et al: L-carnitine suppresses loss of skeletal muscle mass in patients with liver cirrhosis. Hepatol Commun 2: 906-918, 2018.
17. Hiramatsu A, Aikata H, Uchikawa S, Ohya K, Kodama K, Nishida Y, Daijo K, Osawa M, Teraoka Y, Honda F, et al: Levocarnitine use is associated with improvement in sarcopenia in patients with liver cirrhosis. Hepatol Commun 3: 348-355, 2019.
18. Bass NM, Mullen KD, Sanyal A, Poordad F, Neff G, Leevy CB, Sigal S, Sheikh MY, Beavers K, Frederick T, et al: Rifaximin treatment in hepatic encephalopathy. N Engl J Med 362: 1071-1081, 2010.
19. Lyon KC, Likar E, Martello JL and Regier M: Retrospective cross-sectional pilot study of rifaximin dosing for the prevention of recurrent hepatic encephalopathy. J Gastroenterol Hepatol 32: 1548-1552, 2017.
20. Rahimi RS, Brown KA, Flamm SL and Brown RS Jr: Overt hepatic encephalopathy: Current pharmacologic treatments and improving clinical outcomes. Am J Med 134: 1330-1338, 2021.
21. Kumar A, Davuluri G, Silva RNE, Engelen MPKJ, Ten Have GAM, Prayson R, Deutz NEP and Dasarathy S: Ammonia lowering reverses sarcopenia of cirrhosis by restoring skeletal muscle proteostasis. Hepatology 65: 2045-2058, 2017.
22. Kaji K, Saikawa S, Takaya H, Fujinaga Y, Furukawa M, Kitagawa K, Ozutsumi T, Kaya D, Tsuji Y, Sawada Y, et al: Rifaximin alleviates endotoxemia with decreased serum levels of soluble CD163 and mannose receptor and partial modification of gut microbiota in cirrhotic patients. Antibiotics (Basel) 9: 145, 2020.
23. Fujinaga Y, Kawaratani H, Kaya D, Tsuji Y, Ozutsumi T, Furukawa M, Kitagawa K, Sato S, Nishimura N, Sawada Y, et al: Effective combination therapy of angiotensin-II receptor blocker and rifaximin for hepatic fibrosis in rat model of nonalcoholic steatohepatitis. Int J Mol Sci 21: 5589, 2020.
24. Demiroren K, Dogan Y, Kocamaz H, Ozercan IH, Ilhan S, Ustundag B and Bahcecioglu IH: Protective effects of L-carnitine, N-acetylcysteine and genistein in an experimental model of liver fibrosis. Clin Res Hepatol Gastroenterol 38: 63-72, 2014.
25. Horinouchi T, Hoshi A, Harada T, Higa T, Karki S, Terada K, Higashi T, Mai Y, Nepal P, Mazaki Y and Miwa S: Endothelin-1 suppresses insulin-stimulated Akt phosphorylation and glucose uptake via GPCR kinase 2 in skeletal muscle cells. Br J Pharmacol 173: 1018-1032, 2016.
26. Takeda S, Kaji K, Nishimura N, Enomoto M, Fujimoto Y, Murata K, Takaya H, Kawaratani H, Moriya K, Namisaki T et al: Angiotensin receptor blockers potentiate the protective effect of branched-chain amino acids on skeletal muscle atrophy in cirrhotic rats. Mol Nutr Food Res 65: e2100526, 2021.
27. Doyle A, Zhang G, Abdel Fattah EA, Eissa NT and Li YP: Toll-like receptor 4 mediates lipopolysaccharide-induced muscle catabolism via coordinate activation of ubiquitin-proteasome and autophagy-lysosome pathways. FASEB J 25: 99-110, 2011.
28. Girven M, Dugdale HF, Owens DJ, Hughes DC, Stewart CE and Sharples AP: l-Glutamine improves skeletal muscle cell differentiation and prevents myotube atrophy after cytokine (TNF-α) stress via reduced p38 MAPK signal transduction. J Cell Physiol 231: 2720-2732, 2016.
29. Nishikawa H, Shiraki M, Hiramatsu A, Moriya K, Hino K and Nishiguchi S: Japan society of hepatology guidelines for sarcopenia in liver disease (1st edition): Recommendation from the working group for creation of sarcopenia assessment criteria. Hepatol Res 46: 951-963, 2016.
30. Gao JH, Wen SL, Tong H, Wang CH, Yang WJ, Tang SH, Yan ZP, Tai Y, Ye C, Liu R, et al: Inhibition of cyclooxygenase-2 alleviates liver cirrhosis via improvement of the dysfunctional gut-liver axis in rats. Am J Physiol Gastrointest Liver Physiol 310: G962-G372, 2016.
31. Livak KJ and Schmittgen TD: Analysis of relative gene expression data using real-time quantitative PCR and the 2(-Delta Delta C(T)) method. Methods 25: 402-408, 2001.
32. Shahini A, Rajabian N, Choudhury D, Shahini S, Vydiam K, Nguyen T, Kulczyk J, Santarelli T, Ikhapoh I, Zhang Y, et al: Ameliorating the hallmarks of cellular senescence in skeletal muscle myogenic progenitors in vitro and in vivo. Sci Adv 7: eabe5671, 2021.
33. Giusto M, Barberi L, Di Sario F, Rizzuto E, Nicoletti C, Ascenzi F, Renzi A, Caporaso N, D'Argenio G, Gaudio E, et al: Skeletal muscle myopenia in mice model of bile duct ligation and carbon tetrachloride-induced liver cirrhosis. Physiol Rep 5: e13153, 2017.
34. Moretti A, Paoletta M, Liguori S, Bertone M, Toro G and Iolascon G: Choline: An essential nutrient for skeletal muscle. Nutrients 12: 2144, 2020.
35. Sawada Y, Kawaratani H, Kubo T, Fujinaga Y, Furukawa M, Saikawa S, Sato S, Seki K, Takaya H, Okura Y, et al: Combining probiotics and an angiotensin-II type 1 receptor blocker has beneficial effects on hepatic fibrogenesis in a rat model of non-alcoholic steatohepatitis. Hepatol Res 49: 284-295, 2019.
36. Qiu H, Thapaliya S, Runkana A, Yang Y, Tsien C, Mohan ML, Narayanan A, Eghtesad B, Mozdziak PE, McDonald C, et al: Hyperammonemia in cirrhosis induces transcriptional regulation of myostatin by an NF-κB-mediated mechanism. Proc Natl Acad Sci USA 110: 18162-18167, 2013.
37. Saiman Y and Serper M: Frailty and sarcopenia in patients pre- and post-liver transplant. Clin Liver Dis 25: 35-51, 2021.
38. Gao B and Bataller R: Alcoholic liver disease: Pathogenesis and new therapeutic targets. Gastroenterology 141: 1572-1585, 2011.
39. Leung C, Rivera L, Furness JB and Angus PW: The role of the gut microbiota in NAFLD. Nat Rev Gastroenterol Hepatol 13: 412-425, 2016.

40. Rosa CGS, Colares JR, da Fonseca SRB, Martins GDS, Miguel FM, Dias AS, Marroni CA, Picada JN, Lehmann M and Marroni NAP: Sarcopenia, oxidative stress and inflammatory process in muscle of cirrhotic rats-action of melatonin and physical exercise. Exp Mol Pathol 121: 104662, 2021.

41. Thomsen KL, Nielsen SS, Grønbiek H, Flyvbjerg A and Vilstrup H: Effects of lipopolysaccharide endotoxin on the insulin-like growth factor I system in rats with cirrhosis. In Vivo 22: 655-661, 2008.

42. Fang WY, Tseng YT, Lee TY, Fu YC, Chang WH, Lo WW, Lin CL and Lo YC: Triptolide prevents LPS-induced skeletal muscle atrophy via inhibiting NF-κB/TNF-α and regulating protein synthesis/degradation pathway. Br J Pharmacol 178: 2998-3016, 2021.

43. Sawicka AK, Hartmane D, Lipinska P, Wojtowicz E, Lysiak-Szydlowska W and Olek RA: l-Carnitine supplementation in older women. A pilot study on aging skeletal muscle mass and function. Nutrients 10: 255, 2018.

44. Keller J, Couturier A, Haferkamp M, Most E and Eder K: Supplementation of carnitine leads to an activation of the IGF-1/PI3K/Akt signalling pathway and down regulates the E3 ligase MuRF1 in skeletal muscle of rats. Nutr Metab (Lond) 10: 28, 2013.

45. Patel VC, Lee S, McPhail MJW, Da Silva K, Guilly S, Zamalloa A, Witherden E, Støy S, Manakkat Vijay GK, Pons N, et al: Rifaximin-α reduces gut-derived inflammation and mucin degradation in cirrhosis and encephalopathy: RIFSYS randomised controlled trial. J Hepatol 76: 332-342, 2022.

46. Kitagawa R, Kon K, Uchiyama A, Arai K, Yamashina S, Kuwahara-Arai K, Kirikae T, Ueno T and Ikejima K: Rifaximin prevents ethanol-induced liver injury in obese KK-Aʸ mice through modulation of small intestinal microbiota signature. Am J Physiol Gastrointest Liver Physiol 317: G707-G715, 2019.

47. Cellai L, Colosimo M, Marchi E, Venturini AP and Zanolo G: Rifaximin (L/105), a new topical intestinal antibiotic: Pharmacokinetic study after single oral administration of 3H-rifaximin to rats. Chemioterapia 3: 373-377, 1984.